Supporting Information

Deep Metabolomics of a High-Grade Serous Ovarian Cancer Triple Knockout Mouse Model.

Danning Huang[1], David A. Gaul[1], Hongmei Nan[2], Jaeyeon Kim[*,3], Facundo M. Fernández[*,1]

[1]School of Chemistry and Biochemistry, Georgia Institute of Technology, Atlanta, Georgia 30332, United States.

[2]Department of Epidemiology, Richard M. Fairbanks School of Public Health, Indiana University-Purdue University Indianapolis, Indiana University Melvin and Bren Simon Cancer Center, Indianapolis, Indiana, 46202, United States.

[3]Departments of Biochemistry and Molecular Biology, Indiana University School of Medicine, Indiana University Melvin and Bren Simon Cancer Center, Indianapolis, Indiana, 46202, United States.

Table of Contents

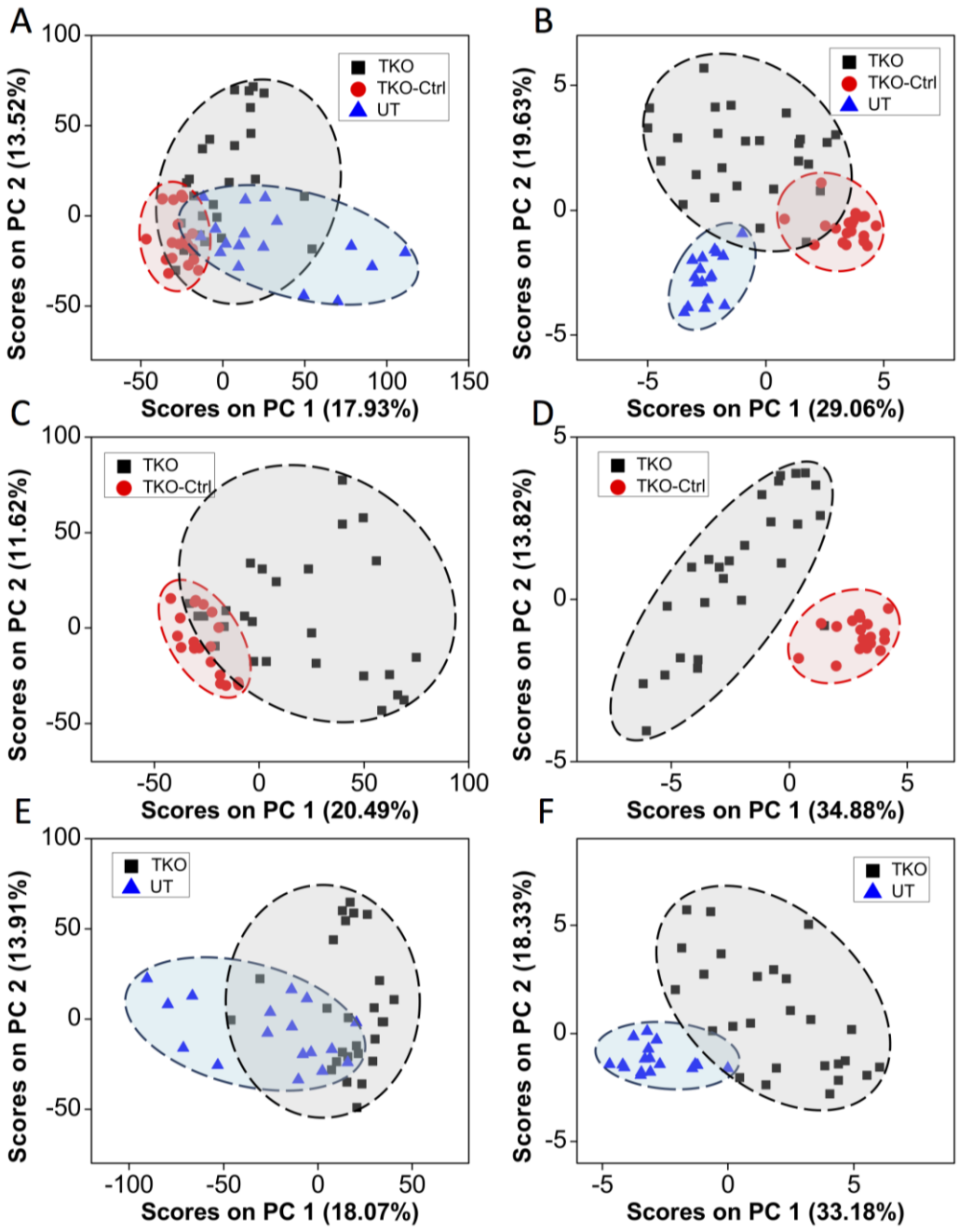

Supplemental Figure S1. PCA score plots of TKO, TKO-Ctrl and UT samples using (A) the initial set of 5937 features and (B) the selected 29-feature panel. The distribution of samples reveals that TKO, TKO-Ctrl and UT samples form distinct clusters, and that more variance between classes is captured across the x-axis using the 29-feature panel. Binary PCA score plots of TKO vs. TKO-Ctrl samples using (C) 5937 features and (D) 29 features, and binary PCA score plots of TKO vs.

UT samples using (E) 5937 features and (F) 29 features. Distinct clustering of TKO and TKO-Ctrl samples, or TKO and UT samples is observed in both binary PCA score plots using the 29-feature panel. For all plots, TKO, TKO-Ctrl and UT samples are represented by black squares, red circles and blue triangles, respectively.

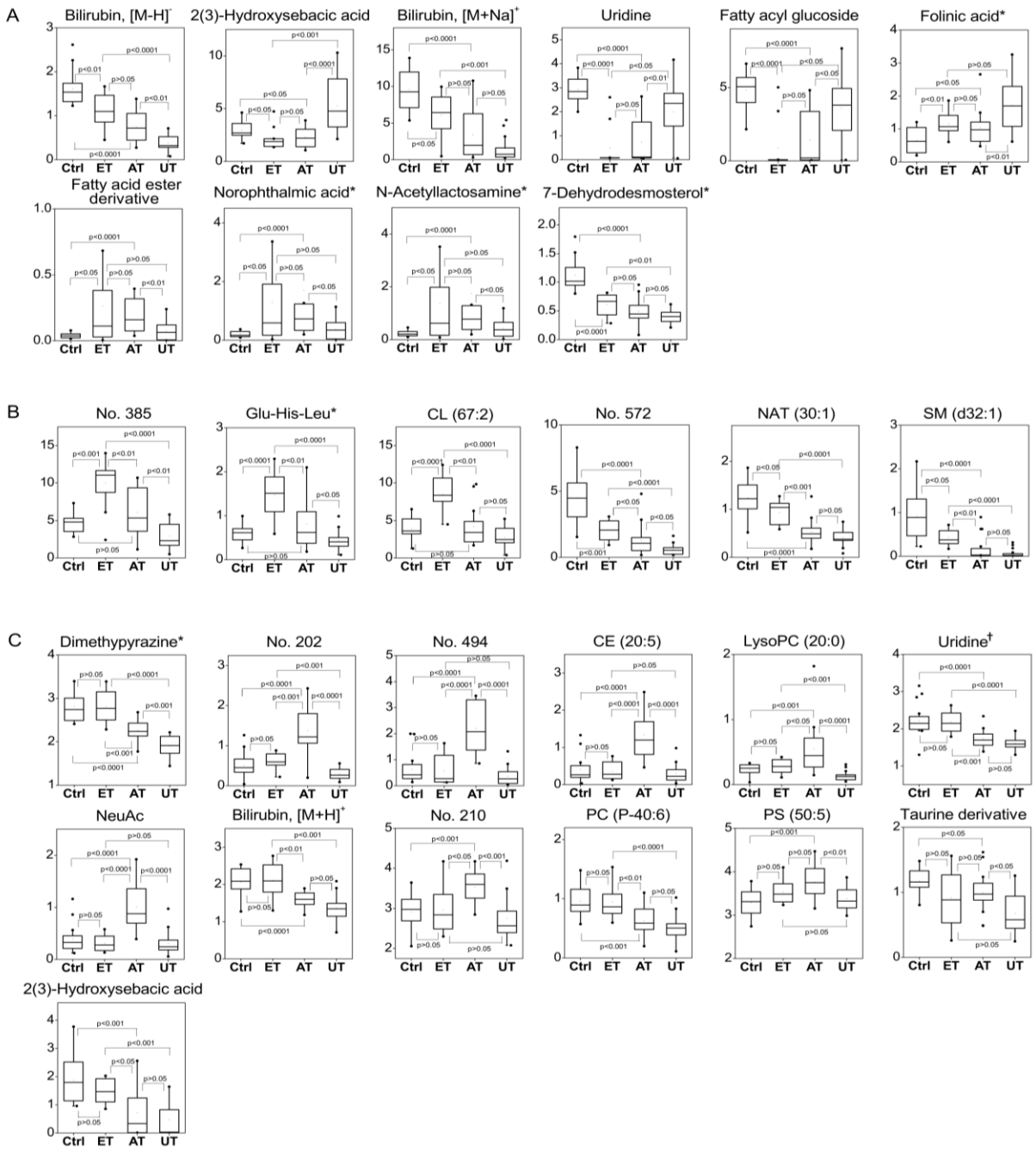

Supplemental Figure S2. Box plots showing changes of the 29 selected spectral features in TKO-Ctrl (n=19), ET (n=10), AT (n=16) and UT samples (n=17). Features are divided into 3 groups showing different trends: (A) group showing different abundances between TKO and TKO-Ctrl/UT, but no significant difference among ET and AT, (B) group showing different abundances between TKO and TKO-Ctrl/UT and also a difference among ET and AT, (C) group where abundances for Ctrl and ET are similar to each other, but, different from AT. The mean, median,

upper and lower quartiles, outliers, and minimum and maximum (whiskers) values are displayed. The p-values were calculated with a Mann-Whitney U test. *Features have isomers; †Feature is an isotopic peak, we attributed this to incomplete de-isotoping of software during data preprocessing. For metabolites without an identity, feature ID numbers are provided.

Table S1. Methods information. (S1a) Chromatographic gradient for RP method: mobile phase A was water/acetonitrile (40:60 v/v), and B was acetonitrile/isopropanol (10:90 v/v). Both mobile phases included 10 mM ammonium formate and 0.1% formic acid additives. (S1b) Chromatographic gradient for HILIC method: mobile phase A was water/acetonitrile (95:5 v/v), with 10 mM ammonium acetate and 0.05% ammonium hydroxide, and B was acetonitrile with 0.05% ammonium hydroxide. Both ionization modes utilized identical mobile phases and identical chromatographic gradients.

(a) **(b)**

RP Separation Method				**HILIC Separation Method**			
Time (min)	**A**	**B**	**Flow rate (ml/min)**	**Time (min)**	**A**	**B**	**Flow rate (ml/min)**
0	60	40	0.4	0	5	95	0.3
1	55	45	0.4	3	63	37	0.3
1.1	50	50	0.4	7	63	37	0.3
5	45	55	0.4	7.1	5	95	0.3
5.1	30	70	0.4	7.2	5	95	0.5
8	1	99	0.4	9.5	5	95	0.5
8.1	60	40	0.4	9.9	5	95	0.3
9.5	60	40	0.4	10	5	95	0.3

Table S2. Summary of MS acquisition parameters.

	Positive Mode	**Negative Mode**
Spray Voltage	3.0 kV	-2.8 kV
Capillary Temperature	275 ° C	275 ° C
Sheath Gas Flow Rate	50	50
Aux Gas Flow Rate	14	14
S-Lens RF Level	40.0	40.0
Probe Heater Temperature	425 ° C	425 ° C

Table S3. Summary of GA variable selection parameters.

Population Size	64
Window Width	1
% Initial Terms (variables)	30
Target Minimum # of Variables	5
Target Maximum # of Variables	30
Penalty Slope	0.01
Max Generations	200
% at Convergence	50
Mutation Rate	0.005
Crossover	Double
Regression Choice	PLS
# of Latent Variables	4
Cross-Validation	Random
# of Splits	6
# of Iterations	10
Replicate Runs	5

Table S4. Detailed MS/MS information for the 29-feature panel that discriminates TKO from TKO-Ctrl and UT samples. The fragment ions listed in the table were obtained using DDA and PRM experiments. The precursor ions that were selected are underlined. Ions in bold are matched to standard spectra or literature spectra. Confidence in the metabolite identities followed four different levels: 1) accurate mass, isotopic abundances, fragmentation spectrum, and retention time of identified compounds matched to standards; 2) accurate mass, isotopic abundances, and fragmentation spectrum matched to databases or consistent with expected fragmentation patterns in literature; 3) accurate mass matched to Lipid Maps, Human Metabolome Database (HMDB) or Metlin database entry, and/or fragmentation showing a few matching characteristic fragment ions, such as lipid head group; and 4) unknown compound.

Feature ID	***CE (eV), Mode***	***Fragment ion m/z***	***ID confidence level***	***Match details (Source)***
208	30 (+)	**<u>109.0764</u>**, **82.0659**, **68.0503**	2	Fragmentation consistent with spectrum (Metlin)
202	30 (+)	<u>271.1148</u>, 253.1043, 230.1402, 213.8154, 209.0921, 140.0342, 139.0501	4	---
385	10 (-)	<u>516.7520</u>, 480.7758, 458.7936, 376.8696, 304.7437, 213.0655, 175.0237, 138.8741, 80.9155	4	---
277	20 (-)	**<u>583.2571</u>**, **285.1244**, **253.1348**, 213.3508	2	Fragmentation consistent with spectrum (Metlin)
494	10 (-)	<u>514.7540</u>, 478.7776, 456.7957, 376.8695, 302.7457, 175.0238, 136.8763, 78.9175	4	---
363	20 (+)	<u>398.2038</u>, 272.1569, 271.1535,	4	---

		255.1586, 165.0908, 133.0858, 120.0890, 119.0856, 89.0602		
427	30 (+)	693.5573, 369.3513, 325,2135, 243.2103, 175.1480, 161.1323, 147.1167, 135.1167, 121.1013, 109.1016, 95.0860	2	Fragmentation consistent with structure
303	20 (+)	**552.4017**, **534.3914**, **369.3360**, **258.1099**, **184.0732**, **104.1074**, **86.0970**	2	Fragmentation consistent with spectrum (Metlin)
751	10 (+)	696.4980, 687.9850, 159.1377	3	Tentative identification based on m/z and isotopic peak patterns
37	30 (-)	217.1076, 199.0971, 185.0811, 167.0704, 141.0910, 123.0804, 113.0232, 85.0646, 69.0333, 57.0332	2	Fragmentation consistent with structure
572	10 (+)	454.8895, 372.8866, 356.9127, 332.8942, 290.8837, 274.9097	4	---
651	30 (-)	**243.0619**, **200.0509**, **140.0340**, **111.0187**, **110.0233**	2	Fragmentation consistent with spectrum (Metlin)
557	10 (-)	**308.0986**, 215.9518, **170.0447**, 119.0337, **87.0074**	2	Fragmentation consistent with spectrum (Metlin)
88	20 (+)	607.2506, 547.3555, 321.1208, 309,1207, 277.1309, 212.8769	2	Fragmentation consistent with structure
274	---	---	3	Tentative identification based

				on m/z and isotopic peak patterns
696	30 (-)	**243.0617**, **200.0556**, **111.0187**, **110.0235**	2	Fragmentation consistent with spectrum (Metlin)
449	---	---	3	Tentative identification based on m/z and isotopic peak patterns
189	30 (+)	**585.2705**, **299.1390**	2	Fragmentation consistent with spectrum (Metlin)
210	10 (+)	619.1966, 559.1757, 537.1939, 500.1024, 456.0761, 362.0945, 280.0915, 207.2064, 104.1073	4	---
98	10 (-)	247.1182, 209.0788, 167.0200, 143.0338, 119.0337, 101,0232, 89.0231, 81.0333	2	Fragmentation consistent with structure
191	30 (+)	818.6043, 184.0734, 125.0000, 86.071	3	Fragmentation consistent with PC headgroup
485	---	---	3	Tentative identification based on m/z and isotopic peak patterns
700	---	---	3	Tentative identification based on m/z and isotopic peak patterns
22	10 (-)	491.3413, 433.2628, 213.2263	3	Accurate mass match

				(Lipid Maps)
644	30 (+)	**276.1190**, **147.0764**, **130.0499**, 115.0392, **102.0554**, **101.0715**, 85.0291, **84.0450**	2	Fragmentation consistent with spectrum (Metlin)
725	10 (-)	219.0187, 176.0126, 149.0015, 124.0062, 80.9639	3	Fragment peaks 124.0062 and 80.9639 match taurine (Metlin)
48	20 (-)	462.0589, 427.0899, 213.2762, 160.8410	3	Accurate mass match (HMDB)
772	30 (-)	**217.1076**, **199.0683**, **181.0858**, 174.9916, **155.1068**, 137.0962, **127.1115**, 96.9589, 83.0489, **59.0125**	2	Fragmentation consistent with spectrum (HMDB)
29	30 (+)	**383.3307**, **95.0861**, **81.0706**	2	Fragmentation consistent with spectrum (Metlin)

Table S5. Sample cohort information. Two repeatedly misclassified samples were collected from a TKO-ET mouse: No. 42, and a UT mouse: No. 68. The oPLS-DA classification model was classifying TKO-ET mouse labeled No.42 as a TKO-Ctrl mouse. This could be due to the age of the mouse, 2.5m when sample was collected, was much younger than the rest of the TKO-ET mice (average age: 4.8m) and close to the average age of the TKO-Pre mice (average age: 2.0m). As TKO-Pre mice were phenotypically closer to the TKO-Ctrl mice, this may explain why the young TKO-ET mouse was classified as a TKO-Ctrl mouse in the models. For the other misclassified sample collected from UT mouse No.68, we couldn't identify the potential reason based on the mice information we had.

	Tail No.	DOB	Color/Ear	Breeding Cage	Genotype p53	Pten	Dicer	Amhr2	Age (days)	Age (Mo)	Dead or collection	Tumor stage	Serum
1	716	10/5/13	Bl/-	PmPtDA29	R172H/+	fl/fl	fl/fl	cre/+	**80**	**2.7**	12/24/13	pre	Y
2	703	10/7/13	Bl/-	PmPtDA33	R172H/+	fl/fl	fl/fl	cre/+	**78**	**2.6**	12/24/13	pre	Y
3	711	10/11/13	Bl/-	PmPtDA36	R172H/+	fl/fl	fl/fl	cre/+	**75**	**2.5**	12/25/13	pre	Y
4	715	10/11/13	Wh/R	PmPtDA36	R172H/+	fl/fl	fl/fl	cre/+	**75**	**2.5**	12/25/13	pre	Y
5	694	10/17/13	Br/-	PmPtDA32	R172H/+	fl/fl	fl/fl	cre/+	**69**	**2.3**	12/25/13	pre	Y
6	695	10/17/13	Br/-	PmPtDA32	R172H/+	fl/fl	fl/fl	cre/+	**69**	**2.3**	12/25/13	pre	Y
7	705	10/17/13	Bl/R	PmPtDA34	R172H/+	fl/fl	fl/fl	cre/+	**69**	**2.3**	12/25/13	pre	Y
8	709	10/19/13	Br/L	PmPtDA35	R172H/+	fl/fl	fl/fl	cre/+	**75**	**2.5**	1/2/14	pre	Y
9	796	10/3/13	Br/R	PmPtDA33	R172H/+	fl/fl	fl/fl	cre/+	**92**	**3.1**	1/3/14	pre	Y
10	860	11/7/13	Br/R	PmPtDA36	R172H/+	fl/fl	fl/fl	cre/+	**57**	**1.9**	1/3/14	pre	Y
11	861	11/7/13	Br/RR	PmPtDA36	R172H/+	fl/fl	fl/fl	cre/+	**57**	**1.9**	1/3/14	pre	Y
12	923	11/28/13	Br/-	PmPtDA33	R172H/+	fl/fl	fl/fl	cre/+	**40**	**1.3**	1/7/14	pre	Y
13	851	11/8/13	Br/R	PmPtDA32	R172H/+	fl/fl	fl/fl	cre/+	**60**	**2.0**	1/7/14	pre	Y
14	855	11/21/13	Br/-	PmPtDA33	R172H/+	fl/fl	fl/fl	cre/+	**47**	**1.6**	1/7/14	pre	Y
15	856	11/21/13	Wh/-	PmPtDA33	R172H/+	fl/fl	fl/fl	cre/+	**47**	**1.6**	1/7/14	pre	Y
16	930	11/25/13	Wh/R	PmPtDA30	R172H/+	fl/fl	fl/fl	cre/+	**44**	**1.5**	1/8/14	pre	Y
17	922	11/28/13	Bl/L	PmPtDA33	R172H/+	fl/fl	fl/fl	cre/+	**41**	**1.4**	1/8/14	pre	Y
18	555	4/26/14	Bl/RL	PmPtDA38	R172H/+	fl/fl	fl/fl	cre/+	**44**	**1.5**	6/9/14	pre	Y
19	568	4/24/14	Bl/R	PmPtDA31	R172H/+	fl/fl	fl/fl	cre/+	**46**	**1.5**	6/9/14	pre	Y
20	571	4/24/14	Bl/RR	PmPtDA31	R172H/+	fl/fl	fl/fl	cre/+	**46**	**1.5**	6/9/14	pre	Y

21	543	4/24/14	Bl/RLR	PmPtDA35	R172H/+	fl/fl	fl/fl	cre/+	**46**	**1.5**	6/9/14	pre	Y	
22	576	4/22/14	Wh/RL	PmPtDA41	R172H/+	fl/fl	fl/fl	cre/+	**48**	**1.6**	6/9/14	pre	Y	22
23	19	12/21/13	Bl/RL	PmPtDA37	R172H/+	fl/fl	fl/fl	+/+	**130**	**4.3**	4/30/14	ctrl	Y	
24	20	12/21/13	Bl/RR	PmPtDA37	R172H/+	fl/fl	fl/fl	+/+	**130**	**4.3**	4/30/14	ctrl	Y	
25	21	12/21/13	Wh/-	PmPtDA37	R172H/+	fl/fl	fl/fl	+/+	**130**	**4.3**	4/30/14	ctrl	Y	
26	91	1/5/14	Bl/-	PmPtDA38	R172H/+	fl/fl	fl/fl	+/+	**115**	**3.8**	4/30/14	ctrl	Y	
27	112	1/8/14	Bl/R	PmPtDA36	R172H/+	fl/fl	fl/fl	+/+	**112**	**3.7**	4/30/14	ctrl	Y	
28	920	11/28/13	Bl/-	PmPtDA37	R172H/+	fl/fl	fl/fl	+/+	**153**	**5.1**	4/30/14	ctrl	Y	
29	925	11/28/13	Br/L	PmPtDA33	R172H/+	fl/fl	fl/fl	+/+	**153**	**5.1**	4/30/14	ctrl	Y	
30	908	12/2/13	Br/RL	PmPtDA33	R172H/+	fl/fl	fl/fl	+/+	**149**	**5.0**	4/30/14	ctrl	Y	
31	911	12/2/13	Bl/R	PmPtDA32	R172H/+	fl/fl	fl/fl	+/+	**149**	**5.0**	4/30/14	ctrl	Y	
32	9	12/10/13	Br/-	PmPtDA34	R172H/+	fl/fl	fl/fl	+/+	**141**	**4.7**	4/30/14	ctrl	Y	
33	4	12/12/13	Br/RL	PmPtDA33	R172H/+	fl/fl	fl/fl	+/+	**139**	**4.6**	4/30/14	ctrl	Y	
34	698	5/18/14	Bl/L	PmPtDA40	R172H/+	fl/fl	fl/fl	+/+	**162**	**5.4**	10/27/14	ctrl	Y	
35	701	5/18/14	Wh/RR	PmPtDA40	R172H/+	fl/fl	fl/fl	+/+	**162**	**5.4**	10/27/14	ctrl	Y	
36	1698	10/7/13	br/-	PmPtDA33	R172H/+	fl/fl	fl/fl	+/+	**91**	**3.0**	1/6/14	ctrl	Y	
37	1700	10/7/13	Br/l	PmPtDA33	R172H/+	fl/fl	fl/fl	+/+	**91**	**3.0**	1/6/14	ctrl	Y	
38	1701	10/7/13	Br/RL	PmPtDA33	R172H/+	fl/fl	fl/fl	+/+	**91**	**3.0**	1/6/14	ctrl	Y	
39	305	2/25/14	Wh/R	PmPtDA37	R172H/+	fl/fl	fl/fl	+/+	**244**	**8.1**	10/27/14	ctrl	Y	
40	303	2/25/14	Bl/-	PmPtDA37	R172H/+	fl/fl	fl/fl	+/+	**244**	**8.1**	10/27/14	ctrl	Y	
41	314	2/23/14	Wh/RL	PmPtDA40	R172H/+	fl/fl	fl/fl	+/+	**246**	**8.2**	10/27/14	ctrl	Y	19
42	710	10/19/13	Br/RL	PmPtDA33	R172H/+	fl/fl	fl/fl	Cre/+	**75**	**2.5**	1/2/14	ET	Y	

43	270	10/18/14	Br/-	PmPtDA35	R172H/+	fl/fl	fl/fl	Cre/+	**172**	**5.7**	4/8/15	ET	Y	
44	263	10/18/14	Bl/R	PmPtDA31	R172H/+	fl/fl	fl/fl	Cre/+	**177**	**5.9**	4/13/15	ET	Y	
45	372	11/11/14	Wh/R	PmPtDA31	R172H/+	fl/fl	fl/fl	Cre/+	**153**	**5.1**	4/13/15	ET	Y	
46	436	11/30/14	Bl/-	PmPtDA39	R172H/+	fl/fl	fl/fl	Cre/+	**136**	**4.5**	4/15/15	ET	Y	
47	378	11/14/14	Bl/L	PmPtDA42	R172H/+	fl/fl	fl/fl	Cre/+	**152**	**5.1**	4/15/15	ET	Y	
48	437	11/30/14	Bl/R	PmPtDA39	R172H/+	fl/fl	fl/fl	Cre/+	**138**	**4.6**	4/17/15	ET	Y	
49	771	2/16/15	Bl/LL	PmPtDA42	R172H/+	fl/fl	fl/fl	Cre/+	**150**	**5.0**	7/16/15	ET	Y	
50	786	2/22/15	Bl/RR	PmPtDA46	R172H/+	fl/fl	fl/fl	Cre/+	**157**	**5.2**	7/29/15	ET	Y	
51	33	2/13/16	Bl/-	TKO4	R172H/+	fl/fl	fl/fl	Cre/+	**122**	**4.1**	6/14/16	ET	Y	10
52	328	10/29/14	Bl/L	PmPtDA41	R172H/+	fl/fl	fl/fl	Cre/+	**172**	**5.7**	4/19/15	LT	Y	
53	319	10/30/14	Bl/RRL	PmPtDA38	R172H/+	fl/fl	fl/fl	Cre/+	**172**	**5.7**	4/20/15	LT	Y	
54	244	10/6/14	Br/R	PmPtDA43	R172H/+	fl/fl	fl/fl	Cre/+	**198**	**6.6**	4/22/15	LT	Y	
55	90	9/1/14	Bl/R	PmPtDA43	R172H/+	fl/fl	fl/fl	Cre/+	**238**	**7.9**	4/27/15	LT	Y	
56	321	10/29/14	Bl/-	PmPtDA39	R172H/+	fl/fl	fl/fl	Cre/+	**181**	**6.0**	4/28/15	LT	Y	
57	276	10/16/14	Bl/L	PmPtDA43	R172H/+	fl/fl	fl/fl	Cre/+	**208**	**6.9**	5/12/15	LT	Y	
58	958	8/2/14	Bl/RL	PmPtDA30	R172H/+	fl/fl	fl/fl	Cre/+	**303**	**10.1**	6/1/15	LT	Y	
59	246	10/6/14	Br/RL	PmPtDA43	R172H/+	fl/fl	fl/fl	Cre/+	**239**	**8.0**	6/2/15	LT	Y	
60	206	5/22/16	bl/-	tko3	R172H/+	fl/fl	fl/fl	Cre/+	**172**	**5.7**	11/10/16	LT	Y	
61	123	8/24/16		tko3	R172H/+	fl/fl	fl/fl	Cre/+	**134**	**4.5**	1/5/17	LT	Y	
62	179	9/2/16		tko11	R172H/+	fl/fl	fl/fl	Cre/+	**130**	**4.3**	1/10/17	LT	Y	
63	312	7/3/16	Bl/L	TKo8	R172H/+	fl/fl	fl/fl	Cre/+	**200**	**6.7**	1/19/17	LT	Y	
64	197	9/2/16		tko11	R172H/+	fl/fl	fl/fl	Cre/+	**150**	**5.0**	1/30/17	LT	Y	

65	97	8/17/16		tko6	R172H/+	fl/fl	fl/fl	Cre/+	**174**	**5.8**	2/7/17	LT	Y	
66	138	8/22/16		tko6	R172H/+	fl/fl	fl/fl	Cre/+	**171**	**5.7**	2/9/17	LT	Y	
67	310	7/3/16	Bl/-	TKo8	R172H/+	fl/fl	fl/fl	Cre/+	**221**	**7.4**	2/9/17	LT	Y	16
68	292	10/21/14	Bl/-	PmfPtA3	fl/fl	fl/fl	+/+	Cre/+	**203**	**6.8**	5/12/15	UT	Y	
69	337	10/28/14	Bl/R	PmfPtA4	fl/fl	fl/fl	+/+	Cre/+	**203**	**6.8**	5/19/15	UT	Y	
70	401	11/10/14	Ag/-	PfPtA10	fl/fl	fl/fl	+/+	Cre/+	**191**	**6.4**	5/20/15	UT	Y	
71	35	2/8/16	Bl/-	cptDKO1	fl/fl	fl/fl	+/+	Cre/+	**185**	**6.2**	8/11/16	UT	Y	
72	40	2/14/16	Bl/R	cptDKO1	fl/fl	fl/fl	+/+	Cre/+	**179**	**6.0**	8/11/16	UT	Y	
73	56	2/28/16	Bl/L	cptDKO1	fl/fl	fl/fl	+/+	Cre/+	**179**	**6.0**	8/25/16	UT	Y	
74	148	4/30/16	Ag/-	cptDKO1	fl/fl	fl/fl	+/+	Cre/+	**123**	**4.1**	8/31/16	UT	Y	
75	117	4/11/16	Ag/-	cptDKO1	fl/fl	fl/fl	+/+	Cre/+	**166**	**5.5**	9/24/16	UT	Y	
76	118	4/11/16	Ag/R	cptDKO1	fl/fl	fl/fl	+/+	Cre/+	**183**	**6.1**	10/11/16	UT	Y	
77	32	7/29/16		cptDKO2	fl/fl	fl/fl	+/+	Cre/+	**126**	**4.2**	12/2/16	UT	Y	
78	258	6/23/16	bl/-	cptDKO2	fl/fl	fl/fl	+/+	Cre/+	**173**	**5.8**	12/13/16	UT	Y	
79	332	7/6/16	bl/R	cptDKO2	fl/fl	fl/fl	+/+	Cre/+	**166**	**5.5**	12/19/16	UT	Y	
80	183	8/29/16		cptDKO2	fl/fl	fl/fl	+/+	Cre/+	**112**	**3.7**	12/19/16	UT	Y	
81	182	8/29/16		cptDKO2	fl/fl	fl/fl	+/+	Cre/+	**133**	**4.4**	1/9/17	UT	Y	
82	246	10/1/16		cptDKO2	fl/fl	fl/fl	+/+	Cre/+	**114**	**3.8**	1/23/17	UT	Y	
83	33	7/29/16		cptDKO2	fl/fl	fl/fl	+/+	Cre/+	**178**	**5.9**	1/23/17	UT	Y	
84	151	8/22/16		cptDKO2	fl/fl	fl/fl	+/+	Cre/+	**162**	**5.4**	1/31/17	UT	Y	17

Additional discussion on the biological roles of identified features not discussed in main manuscript.

One member of the 29-metabolite panel was tentatively identified as a fatty acid ester derivative ($C_{26}H_{52}O_6S$). This metabolite was significantly elevated in TKO mice (Table 1; fold change: +3.03), suggesting this type of fatty acid derivative could be linked to cancer proliferation. Indeed, increased endogenous fatty acid biosynthesis has been reported in ovarian cancer [1], and it is well established that cancer cells have increased *de novo* lipid synthesis to meet the needs of tumor growth, therefore relying on FAs as building blocks for membrane formation, energy storage, and the generation of various signaling molecules [2].

Two compounds in the metabolite panel contained carbohydrate moieties (Table 1): a fatty acyl glucoside ($C_{11}H_{20}O_6$), and an N-acylaminosugar isomer of N-acetyllactosamine. The N-acylaminosugar was detected to be highly increased in serum of TKO mice (Table 1, fold change: 2.78). This increase may be due to an increased release of oligosaccharides from glycoproteins by N-acetylglucosaminidase [3]. In agreement with our observations, Dennis *et al*. found that N-linked oligosaccharides in malignant tumor cells were directly associated with metastatic potential. Inhibition of N-linked oligosaccharide processing in malignant cells results in increased susceptibility to natural immunity, increased cell adhesion, and decreased tumor cell invasion [4]. We also detected decreased serum levels of the $C_{11}H_{20}O_6$ fatty acyl glucoside in TKO mice (Table 1, fold change: -1.98). However, literature searches revealed no mechanism of regulation or biological role of fatty acyl glucosides in ovarian cancer.

Significantly increased serum levels of phosphatidylserine (PS) were detected in TKO mice (Table 1; fold change: +0.16), with higher abundances in TKO-AT mice. Studies have revealed exposed PS as an evolutionarily conserved anti-inflammatory and immunosuppressive signal in the tumor microenvironment [5]. This immunosuppressive effect of exposed PS antagonizes the development of tumor immunity via upregulating immunosuppressive cytokines IL-10 and TGF-β, and suppressing activation of T-cell responses [6], which promotes tumor progression. Elevated PS expression has been reported in human tumor cells [7] and the immunosuppressive effect of PS has been reported in ovarian tumor ascites fluids [6], suggesting PS as a potential therapeutic target for patients with ovarian cancer.

The metabolite with elemental formula $C_{20}H_{23}N_7O_7$ was tentatively identified as 5-formyltetrahydrofolate (folinic acid), or its isomer 10-formyltetrahydrofolate (Table 1). Formyltetrahydrofolate is the formyl derivative of tetrahydrofolic acid, which is an active form of folic acid. Formyltetrahydrofolate is a potent inhibitor of several folate-dependent enzymes and regulates folic acid-dependent one-carbon metabolism [8]. Serum levels of formyltetrahydrofolate were found to be increased in TKO mice (Table 1; fold change: +0.75). It is plausible that formyltetrahydrofolate aids the development of ovarian cancer by increasing purine biosynthesis through one-carbon metabolism [9]. Additionally, Girgis *et al.* found that when folinic acid levels were depleted in human 5Y neuroblastoma cells, these cells displayed a 30-40% decrease in proliferation rates [10].

References

1. Pizer, E.; Wood, F.; Heine, H.; Romantsev, F.; Pasternack, G.; Kuhajda, F., Inhibition of fatty acid synthesis delays disease progression in a xenograft model of ovarian cancer. *Cancer Res* **1996,** *56* (6), 1189-1193.
2. Currie, E.; Schulze, A.; Zechner, R.; Walther, T.; Farese, R., Cellular Fatty Acid Metabolism and Cancer. *Cell Metab* **2013,** *18* (2), 153-161.
3. Tarentino, A. L.; Plummer, T. H., Jr.; Maley, F., The release of intact oligosaccharides from specific glycoproteins by endo-beta-N-acetylglucosaminidase H. *J Biol Chem* **1974,** *249* (3), 818-824.
4. Dennis, J. W., N-linked oligosaccharide processing and tumor cell biology. *Semin Cancer Biol* **1991,** *2* (6), 411-420.
5. Birge, R.; Boeltz, S.; Kumar, S.; Carlson, J.; Wanderley, J.; Calianese, D.; Barcinski, M.; Brekken, R.; Huang, X.; Hutchins, J.; Freimark, B.; Empig, C.; Mercer, J.; Schroit, A.; Schett, G.; Herrmann, M., Phosphatidylserine is a global immunosuppressive signal in efferocytosis, infectious disease, and cancer. *Cell Death Differ* **2016,** *23* (6), 962-978.
6. Kelleher, R. J., Jr.; Balu-Iyer, S.; Loyall, J.; Sacca, A. J.; Shenoy, G. N.; Peng, P.; Iyer, V.; Fathallah, A. M.; Berenson, C. S.; Wallace, P. K.; Tario, J.; Odunsi, K.; Bankert, R. B., Extracellular Vesicles Present in Human Ovarian Tumor Microenvironments Induce a

Phosphatidylserine-Dependent Arrest in the T-cell Signaling Cascade. *Cancer Immunol Res* **2015,** *3* (11), 1269-1278.

7. Utsugi, T.; Schroit, A. J.; Connor, J.; Bucana, C. D.; Fidler, I. J., Elevated expression of phosphatidylserine in the outer membrane leaflet of human tumor cells and recognition by activated human blood monocytes. *Cancer Res* **1991,** *51* (11), 3062-3066.

8. Stover, P.; Schirch, V., The metabolic role of leucovorin. *Trends Biochem Sci* **1993,** *18* (3), 102-106.

9. Fox, J. T.; Stover, P. J., Folate-mediated one-carbon metabolism. *Vitam Horm* **2008,** *79*, 1-44.

10. Girgis, S.; Suh, J.; Jolivet, J.; Stover, P., 5-formyltetrahydrofolate regulates homocysteine remethylation in human neuroblastoma. *J Biol Chem* **1997,** *272* (8), 4729-4734.